

The Optimization of Single Point Incremental Forming (SPIF) to Produce Conical Cups

Ming-Chang Wu*, Yu-Po Liao**, Jyun-Wei Lai***
and Chung-Chen Tsao****

Keywords : single point incremental forming, finite element analysis, Box-Behnken design.

ABSTRACT

Single point incremental forming (SPIF) is an economical and fast sheet metal forming technique, which does not require a set of specified and complicated dies and a press machine. A finite element method (FEM) model of an incremental sheet metal formed conical cup is developed using ABAQUS software. The geometric shape and processing parameters for the punch of the tool path on the thinnest (T) and uniformity (U) of the sidewall thickness of a finished conical cup are measured by SPIF. The SPIF variables for the experimental design include the punch diameter (D), the Z-axis feed-down distance (Z), the rotational speed of the punch (R) and the feed rate (F). The experiment uses 25 sets of analogs and a Box-Behnken design (BBD). Minitab software is used for a regression analysis and to develop the prediction equations for T and U for a finished conical cup. The FEM model and response surface methodology (RSM) are used to determine the optimum design for T and U for a finished conical cup. Compared with the prediction equations for T and U for a finished conical cup that are calculated using RSM, the results from the FEM demonstrate excellent accuracy.

Paper Received July, 2022. Revised August, 2023. Accepted November, 2023. Author for Correspondence: Chung-Chen Tsao.

* Associate professor, Department of Mechanical Engineering, Lunghwa University of Science and Technology, Taoyuan, Taiwan 333326, ROC.

** Graduate student: Department of Mechanical Engineering, National Central University, Taoyuan, 32054, Taiwan, R.O.C.

*** Graduate student: Department of Mechanical Engineering, Lunghwa University of Science and Technology, Taoyuan, Taiwan 333326, ROC

**** Professor, Department of Mechanical Engineering, Lunghwa University of Science and Technology, Taoyuan, Taiwan 333326, ROC.

INTRODUCTION

The demand for environmentally friendly manufacturing processes is witnessing an increase in government regulations, as well as customer perceptions on environmental issues impacting decisions on product purchases. Sheet metal processing, which does not produce chips during forming, is a traditional machining process.

The quantity and quality of finished products that are produced using sheet metal processing has gradually become small, diverse, customized and requires precise manufacturing and development. Single point incremental forming (SPIF) is used in industry to decrease the manufacturing cost and to increase machining efficiency. A round-tipped punch moves along a pre-defined path to produce an open-formed surface product, as shown in Fig. 1. SPIF studies focus on the forming method (Ambrogio et al., 2012; Fan et al., 2008; Fan and Gao, 2014; Jeswiet et al., 2005; Li et al., 2015; Martins et al., 2008; Petek et al., 2009; Silva et al., 2008), the tool path (Azaouzi and Lebaal, 2012; Duflou et al., 2007; Hagan and Jeswiet, 2004; Ham and Jeswiet, 2006; Hamilton and Jeswiet, 2010; Lasunon, 2013; Lu et al., 2013; Yamashita et al., 2008) and the finished wall thickness for a product (Ambrogio et al., 2005; Duflou et al., 2008; Essa, 2011; Verbert et al., 2008). However, an uneven sidewall thickness that results from the complex forming stresses between the punch and the workpiece is a defect of SPIF. Petek et al. demonstrated that the rotational speed of the punch and the state of the lubricant have little effect on the maximum stress, but have a significant effect on surface quality. Li et al. used finite element analysis (FEA) for SPIF for cones and showed that the deformation of the plate during the forming process is mainly affected by the combined stress of stretching, bending and shearing. Ham and Jeswiet determined the maximum limit of the inclination angle for the finished product for different processing conditions (the sheet thickness, the step-size and the punch diameter). They showed that for the same processing conditions, a thicker sheet allows a greater

inclination limit for the finished product and that the inclination limit for forming is reduced if a larger punch is used. Yamashita et al. used FEA to determine the effect of step-size, punch path and feed rate on sheet forming for SPIF and showed that if the feed rate is too fast, a stepped pattern is produced on the inner wall of the finished product. Lu et al. used path planning to calculate the contour density using the scallop height and then interpolated the contour line to create a continuous spiral oblique path. The pits and tracks that are generated also produce a more accurately sized finished product. Ambrogio et al. used finite elements (FEs) to determine the distribution of the thickness for products that are produced using SPIF and showed that increasing the step-size decreases the thickness of the finished product. Duflou et al. (2007) and Verbert et al. showed that the thickness of the sheet after SPIF can be roughly estimated using the sine law to determine an average approximate value. During SPIF, the sheet-metal is firmly clamped between the back-plate and the pressure plate to prevent plastically sliding, so the thickness of the finished sidewall after SPIF can be uneven (Ambrogio et al., 2005; Duflou et al., 2008; Essa, 2011; Ham and Jeswiet, 2006; Verbert et al., 2008; Yamashita et al., 2008).

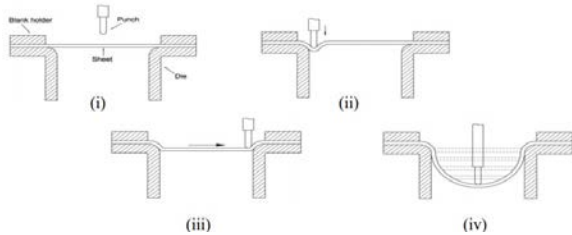


Fig. 1. Diagram for SPIF: (i) the undeformed stage of the initial unprocessed sheet; (ii) the punch contacts the sheet and feeds to the depth of the first incremental point; (iii) the punch is horizontally fed in the longitudinal and latitudinal directions at each increment in depth and (iv) the final product is formed

Response surface methodology (RSM) is used for analysis and for solving procedures (Lianget al., 2021; Shim, 2021; Vijayakumar et al., 2020; Zeng et al., 2009). It is used to produce the optimal product design or process parameters for scientific systems or industrial applications, especially if the system characteristics are affected by a large number of variables. A Box-Behnken design (BBD) is commonly used in combination with RSM to produce the optimal quality for a target. Song et al. used an analysis of variance (ANOVA) with a BBD to determine the significance of independent parameters and interactions (Song et al., 2021). To produce a greater value of the thinnest (T) and uniformity (U) for the SPIF process, a finite element method (FEM) and a design of experiment were used to optimize the

design for an axisymmetric conical cup for SPIF. The experiment uses 25 sets of analogs and a BBD. Minitab software is used for regression analysis and to develop the prediction models for T and U . The FEM model and RSM are used to determine the optimum design that produces the best value for T and U .

METHOD AND EXPERIMENT

FEA

In order to reduce the cost and efficiency of the experiment, this study uses the experimental results of the SPIF axisymmetric conical cup in the previous literature (Essa, 2011) as verification data. The design of the fixture for SPIF is shown in Fig. 2. The diameter of the punch is 15 mm. The inner diameter of conical cup is 150 mm, and the thickness of the back-plate and the pressure plate is 10 mm each. The sheet is aluminum alloy (Al-5251-H22) and the workpiece measures of $170 \times 170 \times 1 \text{ mm}^3$. The plastic behavior of the material is assumed to be isotropic, with a stress-strain curve of $\bar{\sigma} = 390(\bar{\epsilon})^{0.19}$ (MPa), where $\bar{\sigma}$ is the flow stress and $\bar{\epsilon}$ is the plastic strain. For simplicity, anisotropic, thermal and rate effects are not included in the current model. The data of the FEM model are shown in Table 1. The final product has an upper diameter of 90 mm, a lower diameter of 20 mm, a height of 35 mm and a wall angle of 45° . The SPIF axisymmetric conical cup is produced using a clockwise stepped tool path, as shown in Fig. 3. The starting position for the punch is at coordinates (45, 0, 0), the rotational speed of the punch is 0 rpm, the feed rate is 30 mm/s, the step-over length is 0.25 mm and the step-down distance in the Z-axis direction is 1 mm. The Coulomb friction coefficient (μ_p) between the punch and the workpiece is 0.05 (Essa, 2011). The workpiece is firmly fixed between the bearing plate and the pressing plate to prevent sliding.

Table 1. The data of the FEM model

Workpiece	Young's modulus	Poisson ratio	Initial yield stress	Density
Al-5251-H22	70 GPa	0.34	165 MPa	2,700 kg/m^3 .

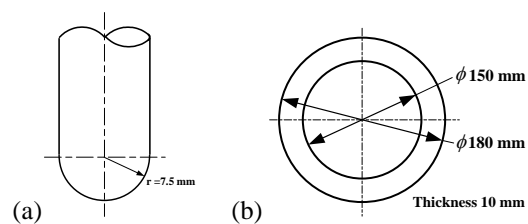


Fig. 2. (a) Punch and (b) Back-plate and pressure plate (mm)

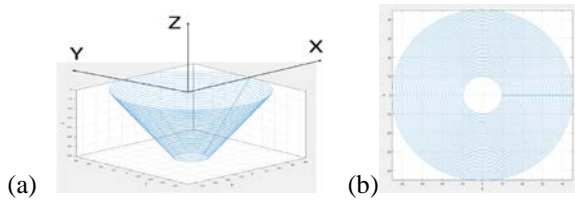


Fig. 3. Punch using a clockwise stepped tool path: (a) Isometric projection and (b) X-Y Front view

Many studies show that a product that is produced using SPIF has an uneven distribution the thickness F (Ambrogio et al., 2005; Duflou et al., 2008; Essa, 2011; Ham and Jeswiet, 2006; Verbert et al., 2008; Yamashita et al., 2008). The upper half sidewall of the finished conical cup is the thinnest. To determine the sidewall thickness for the finished conical cup, the result of the ABAQUS analysis is used to cut the formed conical cup along the X-axis through the center point, as shown in Fig. 4. When a conical cup section is produced, the path that is formed by all grids from the sheet boundary to the center point is determined and the measurement function of ABAQUS is used to calculate the thickness distribution data for the sheet section, as shown in Fig. 5. Fig. 5 shows that the cross-sectional thickness of the finished conical cup is non-uniform between 100 to 118 mm in the X-axis direction on the right sidewall. The sidewall is thinnest (0.6263 mm) at 118 mm in the X-axis direction, which is shown as point A in Fig. 4. The uniformity of the cross-sectional thickness of the finished conical cup is calculated using the covariance of variation (CV), which is defined as:

$$CV = s / \tilde{x} \quad (1)$$

where

$$s = \sqrt{\frac{\sum_{i=1}^N (x_i - \tilde{x})^2}{N-1}}$$

$$\tilde{x} = \frac{\sum_{i=1}^N x_i}{N}$$

where x_i is the sheet thickness of point i , N is the number of statistical samples, s is the standard deviation and \tilde{x} is the average value of the sheet thickness. The smaller the value of CV (U) in Eq. (1), the more uniform is the thickness of the cross-section.

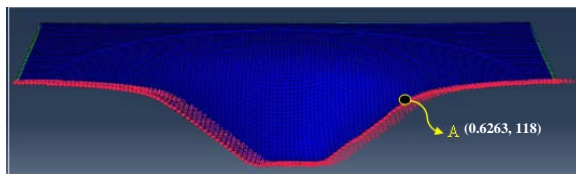


Fig. 4. X-axis sectional view

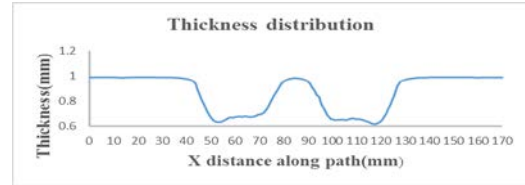


Fig. 5. Sheet thickness for the X-axis section

To determine the values of T and U for the finished conical cup, this study begins by using 5,000 grids and this number is increased in increments of 5,000. The convergence of the numerical calculation results is used to select the most suitable grid for the FE simulation. As shown in Figs. 6 and 7, the values of T and U converge if 25,000 grids are used, so 25,000 grids were used for the FEA and the experimental regression analysis. Fig. 8 compares the theoretical and experimental results for the thickness and profile of a finished conical cup with those for a previous study (Essa, 2011). The thickness and profile of the finished conical cup for the previous study (Essa, 2011) are in good agreement with the values that are obtained by this study. A FEA model was used and RSM to determine the optimal parameters for predicting the thinnest and most uniform sidewall that is possible for SPIF.

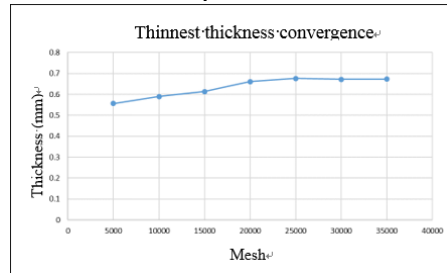


Fig. 6. Mesh convergence analysis to determine the thinnest possible sidewall

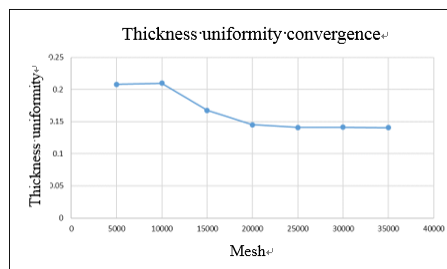
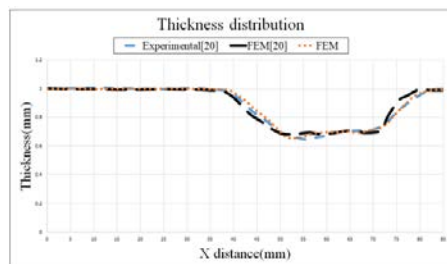
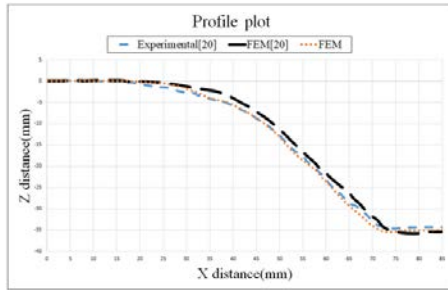


Fig. 7. Mesh convergence analysis for uniformity of sidewall thickness



(a) Thickness distribution



(b) Profile plot

Fig. 8. Numerical and experimental values for thickness distribution and profile for the sidewall

thickness gauge with an accuracy of 0.001mm was used for measurement (Qualitot-21752, China).



Fig. 9. Photograph of the experimental setup

BBD

The quality characteristics (T and U) were determined for the SPIF of finished conical cups. The punch diameter D (mm), the rotational speed of the punch R (rpm), the Z -axis feed-down distance Z (mm) and the feed rate F (mm/s) are the factors for forming. To obtain the values for T and U , a four-factor design with three distinct levels is used, as shown in Table 2. The levels for the factors are represented by the coding variables -1, 0 and 1, which values represent the punch diameter and processing parameters for the study by Essa. The maximum value for each factor level is 1, the minimum value is -1 and the median value is 0.

Table 2. Quality factor variables and natural variables

Level	Punch diameter D (mm)	Punch rotational speed R (rpm)	Z -axis step-down distance Z (mm)	Feed rate F (mm/s)
1	19	2,000	2.0	40
0	17	1,000	1.5	35
-1	15	0	1.0	30

Experiment

A workpiece (Al-5251-H22 aluminum alloy) was used that is 1.0 mm thick. The confirmation experiments for SPIF were conducted three times, using a Tongtai TMV-850QII machining center. A photograph of the experimental setup is shown in Fig. 9. The punch tool is clamped in the CNC tool holder and controlled using G-code. The Z -axis loads during SPIF were measured using a Kistler 9170A rotary piezoelectric dynamometer, measures the Z -axis load that is exerted by the punch tool on the workpiece. The dynamometer outputs the tiny voltage that is generated by the punch tool as an analog signal. The charge is transferred to the charge amplifier (Kistler Type 5238B) through the proximity sensor (Kistler Type 5236B) and the data acquisition device (Kistler Type 5697). A charge amplifier then converts this value into a voltage signal using an analog/digital interface. The card converts the voltage signal into the Z -axis load and stores it in the computer hard disk and uses the application software to calculate the Z -axis load for SPIF. The thickness of the workpiece changes only slightly after SPIF, so a digital

RESULTS AND DISCUSSION

Factor analysis

The relationship between the coding variables and the natural variables and the simulation results is shown in Table 3. Statistical software (Minitab 14) is used to calculate the regression coefficients and for the ANOVA. The significance of the coefficients is tested at a 95% confidence level to determine the model terms that have the greatest effect on the model. The regression models for T (y_1^B) and U (y_2^B) use a full second-order polynomial in terms of four input variables and the significance is determined using the T-value. The larger the T-value, the more significant is the model. Eqs. (2) and (3) show the respective regression equations for y_1^B and y_2^B .

$$y_1^B = 0.5918 - 0.031225D - 0.02015R - 0.029167Z - 0.023392F - 0.008196D^2 - 0.014758R^2 - 0.004583Z^2 - 0.005096F^2 + 0.01175D \times R + 0.017425D \times Z + 0.0179D \times F + 0.02085R \times Z + 0.0127R \times F - 0.000975Z \times F \quad (2)$$

$$y_2^B = 0.1451 + 0.010792D + 0.001025R + 0.005967Z - 0.0051F - 0.001125D^2 + 0.001725R^2 - 0.000038Z^2 + 0.01562F^2 + 0.00375D \times R + 0.00425D \times Z + 0.001875D \times F + 0.002425R \times Z + 0.00275R \times F + 0.002025Z \times F \quad (3)$$

Table 3. Results for the BBD

No	D	R	Z	F	T (mm)	U
1	1	1	0	0	0.5319	0.1605
2	1	-1	0	0	0.5531	0.1503
3	-1	1	0	0	0.5746	0.1325
4	-1	-1	0	0	0.6428	0.1373
5	1	0	1	0	0.5421	0.1651
6	1	0	-1	0	0.5625	0.1461
7	-1	0	1	0	0.5604	0.1333
8	-1	0	-1	0	0.6505	0.1313
9	1	0	0	1	0.5324	0.1528
10	1	0	0	-1	0.5434	0.1603
11	-1	0	0	1	0.5646	0.1281
12	-1	0	0	-1	0.6472	0.1431
13	0	1	1	0	0.5401	0.1521
14	0	1	-1	0	0.5621	0.1411
15	0	-1	1	0	0.5279	0.1584
16	0	-1	-1	0	0.6333	0.1377

17	0	1	0	1	0.5278	0.1489
18	0	1	0	-1	0.5691	0.1528
19	0	-1	0	1	0.5491	0.1385
20	0	-1	0	-1	0.6412	0.1534
21	0	0	1	1	0.5484	0.1438
22	0	0	1	-1	0.5733	0.1578
23	0	0	-1	1	0.6025	0.1384
24	0	0	-1	-1	0.6313	0.1443
Centre	0	0	0	0	0.5918	0.1451

Fig. 10 shows the effect of the four input variables at various levels on T . It can be seen from Fig. 10 that D is the most important influencing parameter in SPIF, followed by Z , F and R . The decrease in D causes the contact stress increase. Decreasing the R can avoid excessive frictional contact between the punch and the workpiece, which causes the temperature of the material at the punch contact point to rise, and the material to quickly soften locally. Hence, a decrease R in both punch and workpiece increases forming quality on T . It is observed that as Z and F decrease, the forming quality on the T continues to increase, due to the less energy input during SPIF.

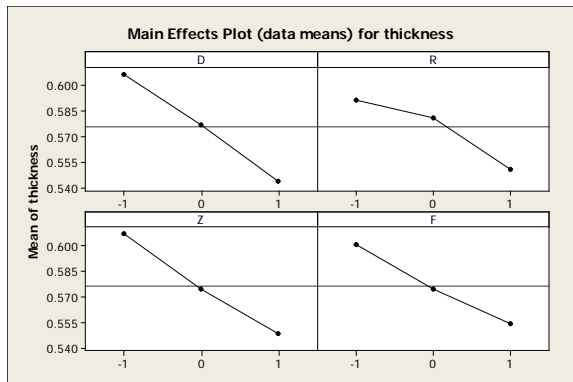


Fig. 10. Effect of the four input variables at various levels on T

The regression analysis and ANOVA results for the value of T for a 95% confidence level are shown in Table 4. The determination coefficient for the model for T is $R^2=0.955$ and the F-ratio is 15.19. The value of R^2 shows that the control factors account for 95.5 % of the variation in the value of T and only 4.5 % of total variation cannot be described by the quadratic model. This result shows that the model is largely significant. Table 3 shows that all of the input variables (D , R , Z and F) have a P-value of less than 0.05, so all input process parameters are significant for the value of T . The results in Table 4 also show that the first-order interaction factors ($D \times Z$, $D \times F$ and $R \times Z$) have a significant effect on the value of T . Fig. 11 shows a 3D surface view of the first-order interaction factors ($D \times Z$, $D \times F$ and $R \times Z$). The maximum value of T occurs for the lower values of these first-order interaction factors at $D=15$ mm (-1), $Z=1.0$ mm (-1), $F=30$ mm/s (-1) and $R=0$ rpm (-1).

Therefore, as D , Z , F and R decreases, the value of T increases and changes in the first-order interaction factors for T are nonlinear.

Table 4. Regression analysis results for the value of T using a BBD

R^2	0.955				
R^2_{adj}	0.892				
Standard error	0.0147843				
Number of observations	25				
ANOVA	Degrees of freedom	Variance	Square error	F-ratio	P-value
Regression	14	0.039564	0.002826	15.19	6.69E-5
Residual	10	0.001860	0.000186		
Sum	24	0.041424			
	Coefficient	Standard error	T-value	P-value	Sig.
Constant	0.5918	0.013639	43.389	0.000	Sig.
D	-0.031225	0.003937	-7.930	0.000	Sig.
R	-0.02015	0.003937	-5.118	0.000	Sig.
Z	-0.029167	0.003937	-7.408	0.000	Sig.
F	-0.023392	0.003937	-5.941	0.000	Sig.
$D \times D$	-0.008196	0.008117	-1.010	0.336	
$R \times R$	-0.014758	0.008117	-1.818	0.099	
$Z \times Z$	-0.004583	0.008117	-0.565	0.585	
$F \times F$	-0.005096	0.008117	-0.628	0.544	
$D \times R$	0.001175	0.00682	1.723	0.116	
$D \times Z$	0.017425	0.00682	2.555	0.029	Sig.
$D \times F$	0.01790	0.00682	2.625	0.025	Sig.
$R \times Z$	0.02085	0.00682	3.057	0.012	Sig.
$R \times F$	0.01270	0.00682	1.862	0.092	
$Z \times F$	-0.000975	0.00682	0.143	0.889	

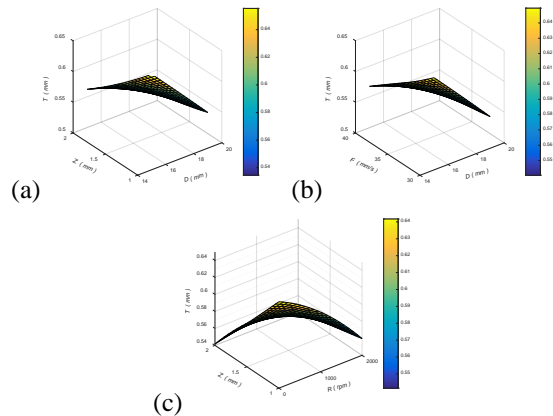


Fig. 11. 3D surface view of the first-order interaction factors: (a) $D \times Z$, (b) $D \times F$ and (c) $R \times Z$

Fig. 12 shows the effect of the four input variables at various levels on U . D is the parameter that has the greatest effect on SPIF, followed by Z , F and R . The effect of the four input variables on the value of U is similar. An increase in D increases the contact zone between the punch and the workpiece so the values of Z and R increase and more energy is input. This produces a decrease in the value of U , which increases the processing quality of SPIF products. However, R does not have an insignificant effect on the value of U for SPIF. A smaller value for F also decreases the input energy for the punch.

The results in Table 5 show that the first-order interaction factors ($D \times R$, $D \times Z$ and $R \times F$) have a significant effect on the value of U . Fig. 13 shows a 3D surface view of the first-order interaction factors

($D \times R$, $D \times Z$ and $R \times F$). Figs. 13 (a) and (b) show that the minimum value for U occurs for values of these first-order interaction factors ($D \times R$ and $D \times Z$) of $D=15$ mm (-1), $Z=1.0$ mm (-1) and $R=2,000$ rpm (1). Fig. 12 (c) shows that the minimum value of U occurs for values of the first-order interaction factors ($R \times F$) of $R=0$ rpm (-1) and $F=40$ mm/s (1). Therefore, as F increases and R decreases, the value of U decreases and changes in these first-order interaction factors for U are also nonlinear.

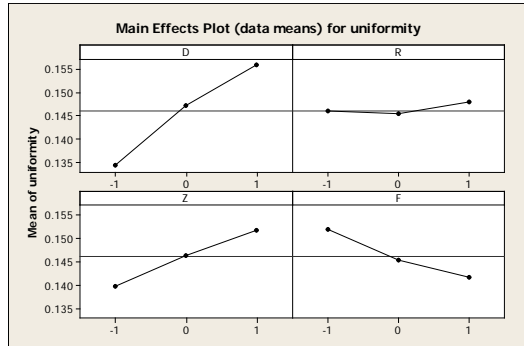


Fig. 12. The effect of the four input variables at various levels on U

The regression analysis results for the value of U are shown in Table 5. The determination coefficient for the model for U is $R^2=0.978$ and the F-ratio is 31.03. The factor confidence level is 95%, so a P-value of less than 0.05 means that a factor is insignificant. The value of R^2 shows that the control factors account for 97.8 % of the variation in U and only 2.2 % of the total variation is not described by the quadratic model. These results for the model are largely significant. The results in Table 5 show that all of the input variables have a P-value of less than 0.05 except R . Therefore, D , Z and F have a significant effect on the value of U .

Table 5. Regression analysis results for U using a BBD

ANOVA		Degrees of freedom	Variance	Square error	F-ratio	P-value
R^2			0.978			
R^2_{adj}			0.946			
Standard error			0.0023541			
Number of observations			25			
Regression	14	0.002408	0.000172	31.03	2.38E-6	
Residual	10	0.000055	0.000006			
Sum	24	0.002463				
	Coefficient	Standard error	T-value	P-value	Sig.	
Constant	0.14510	0.002354	61.638	0.000	Sig.	
D	0.010792	0.000680	15.880	0.000	Sig.	
R	0.001025	0.000680	1.508	0.162		
Z	0.005967	0.000680	8.780	0.000	Sig.	
F	-0.005100	0.000680	-7.505	0.000	Sig.	
$D \times D$	-0.001125	0.001401	-0.803	0.441		
$R \times R$	0.001725	0.001401	1.231	0.246		
$Z \times Z$	-0.00038	0.001401	-0.027	0.979		
$F \times F$	0.001562	0.001401	1.115	0.291		
$D \times R$	0.003750	0.001177	3.186	0.010	Sig.	
$D \times Z$	0.004250	0.001177	3.611	0.005	Sig.	
$D \times F$	0.001875	0.001177	1.593	0.142		

$R \times Z$	-0.002425	0.001177	-2.060	0.066	
$R \times F$	0.002750	0.001177	2.336	0.042	Sig.
$Z \times F$	-0.002025	0.001177	-1.720	0.116	

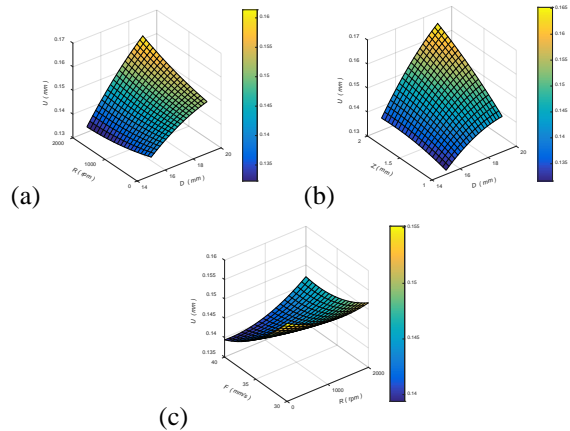


Fig. 13. 3D surface view of the first-order interaction factors: (a) $D \times R$, (b) $D \times Z$ and (c) $R \times F$

Optimization analysis

Four input variables were used to determine the optimal quality characteristics (response T and U) for a finished conical cup. The value of T has a larger-the-better characteristic and the value of U has a smaller-the-better characteristic. The optimum parameter settings for T and U are shown in Table 6. The optimum settings are contradictory for the two responses so a different method of optimization is required.

Table 6. The optimum parameters settings for T and U

Response	Optimal parameters
T	$D_{-1}Z_{-1}R_{-1}F_{-1}$
U	$D_1Z_1R_0F_{-1}$

It is easier to determine the value of T than to determine the value of U , so the value of T is used to optimize the quality characteristic (response) to produce a lesser value for U . The geometry (D) and the forming process parameters (Z , R and F) that are shown in Table 2 are used to optimize the value of T . The optimal solution must satisfy the limiting condition for an objective function, which is:

$$\begin{cases} \text{Objective function: Max } Y_{15} \\ \text{Limiting condition: Min } Y_{25} \end{cases} \quad (4)$$

where Y_{15} is the regression model for T (Eq. (2)) and Y_{25} is the regression model for U (Eq. (3)). Using Eq. (4) to determine the conditions for the input variables for the values of T and U , the optimal conditions for the quality characteristics that are calculated by Minitab software are shown in Table 7. The optimized rotational speed for the punch is 1.70 rpm. The servo motor encoder in the machining center machine does not generate speed of less than 100 rpm so the optimum rotational speed for the punch of the confirmation experiment is 0 rpm. Using the modified optimal values in Table 7, the simulation

and confirmation experiments were performed to verify the accuracy of the prediction model and the results are shown in Table 8. The respective values of T and U for the FEM are 0.6398 and 0.1331. A comparison of the theoretical simulation value and the predictive and experimental results using the regression models (Eqs. (2) and (3)) and the confirmation experiment shows that the respective percentage errors for the T and U are 1.72 % and 1.88 %, and 2.26 % and 3.01%. Fig. 14 shows a photograph of a finished conical cup. Fig. 15 shows the correlation between the Z-axis load and the forming time. As the Z-axis load increases to 1,100N during forming, a stable is achieved for SPIF. The period of the fluctuation on the Z-axis load also decreases gradually because the SPIF path for each pass decreases as the Z-axis step-down distance increases so the contact area between the punch tool and the workpiece also increases as the Z-axis step-down distance increases. Table 9 compares the optimized solutions of T and U in the FEM model between this study and Essa. These results show that the optimized solutions of T and U for the FEM model in this study are better than those of Essa. Fig. 16 shows the optimized solution, which gives a significantly smaller value for U for SPIF.

Table 7. Ideal and modified optimal settings for the input variables

Mode	Punch diameter D (mm)	Punch rotational speed R (rpm)	Z-axis step-down distance Z (mm)	Punch feed rate F (mm/s)
Ideal	15 (-1)	1.70 (-0.9983)	1.0 (-1)	38.77 (0.7534)
Modified	15 (-1)	0 (-1.0)	1.0 (-1)	38.77 (0.7534)

Table 8. Comparison of the FEM, predicted and experimental values for T and U

Type	T (mm)	Error (%)	U	Error (%)
FEM	0.640	-	0.133	-
Predicted	0.651	1.72	0.130	2.26
Experiment	0.652	1.88	0.137	3.01

Table 9. Comparison of the optimized solutions of T and U in the FEM model between this study and Essa

	T (mm)	U
Essa	0.6263	0.1384
This study	0.640	0.133

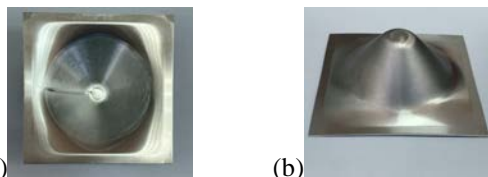


Fig. 14. A photograph of a finished conical cup (a):upward view and (b) downward view

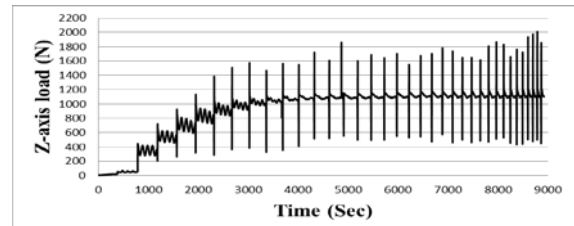


Fig. 15. Correlation between the Z-axis load and the forming time

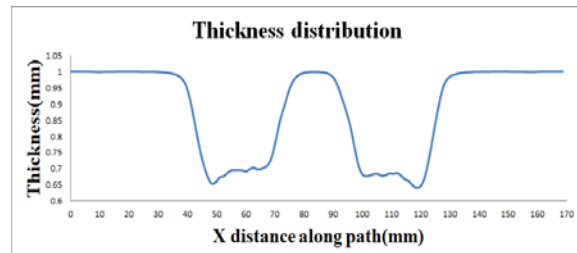


Fig. 16. Thickness distribution using optimal settings for the input variables

CONCLUSIONS

A FEM was used to simulate the processing conditions for SPIF. RSM is used to establish two optimized mathematical models for T and U . This results allow the following conclusions to be drawn:

1. The values of D , Z and F have a more significant effect and the value of R has the smallest effect on the value of T for a conical cup that is produced using SPIF. The smaller the values of D , R , Z and F , the better is the value of T .
2. In terms of the thickness uniformity for a finished conical cup that is produced using SPIF, the values of D , Z and F have a more significant effect and the value of R has the smallest effect. The larger the values of D and Z and the lower the value of F , the better is the value of U .
3. The value of R at the center point of the punch is 0 so it is easy to produce the least uniform T . However, the values of T and U for the section are better in the diagonal direction.

The modified optimization factor coding variable levels are a punch diameter (D)=-1 (15 mm), a punch rotational speed (R)= -1 (0 rpm), a Z-axis feed-down distance (Z)=-1 (1.0 mm) and a feed rate (F)=0.7534 (38.77 mm/s) in SPIF. The respective values of T and U for the FEM for the finished product are 0.6398 mm and 0.1331. The percentage error for the regression models and the confirmation experiment for the values of T and U are 1.72 % and 1.88 %, and 2.26 % and 3.01%.

ACKNOWLEDGMENT

Financial support for this work was provided by the National Science Council Taiwan, R.O.C, under

the contract MOST 108-2221-E-262-002-MY2.

REFERENCES

- Ambrogio, G., Filice, L., Gagliardi, F., and Micari, F., "Sheet Thinning Prediction in Single Point Incremental Forming." *Adv. Mater. Res.*, Vols. 6-8, pp. 479-486 (2005).
- Ambrogio, G., Filice, L., and Gagliardi, F., "Formability of Lightweight Alloys by Hot Incremental Sheet Forming." *Mater. Des.*, Vol. 34, pp. 501-508 (2012).
- Azaouzi, M., and Lebaal, N., "Tool Path Optimization for Single Point Incremental Sheet Forming Using Response Surface Method." *Simul. Model. Pract. Theory*, Vol. 24, pp. 49-58 (2012).
- Duflou, J., Tunckol, Y., Szekeres, A., and Vanherck, P., "Experimental Study on Force Measurements for Single Point Incremental Forming." *J. Mater. Process. Technol.*, Vol. 189, pp. 65-72 (2007).
- Duflou, J.R., Callebaut, B., Verbert, J., and De Baerdemaeker, H., "Improved SPIF Performance Through Dynamic Local Heating." *Inter. J. Mach. Tools Manuf.*, Vol. 48, pp. 543-549 (2008).
- Essa, K., "Finite Element Prediction of Deformation Mechanics in Incremental Forming Processes." Ph. D. Thesis, School of Mechanical Engineering, The University of Birmingham Edgbaston, UK (2011).
- Fan, G.Q., Gao, L., Hussain, G., and Wu, Z.L., "Electric Hot Incremental Forming: A Novel Technique." *Int. J. Mach. Tools Manuf.*, Vol. 48, pp. 1688-1692 (2008).
- Fan, G.Q., and Gao, L., "Mechanical Property of Ti-6Al-4V Sheet in One-Side Electric Hot Incremental Forming." *Inter. J. Adv. Manuf. Technol.*, Vol. 72, pp. 989-994 (2014).
- Hagan, E., and Jeswiet, J., "Analysis of Surface Roughness for Part Formed by Computer Numerical Controlled Incremental Forming." *J. Eng. Manuf.*, Vol. 218, pp. 1307-1312 (2004).
- Ham, M., and Jeswiet, J., "Single Point Incremental Forming and the Forming Criteria for AA3003." *CIRP Ann. – Manuf. Technol.*, Vol. 55, No. 1, pp. 241-244 (2006).
- Hamilton, K., and Jeswiet, J., "Single Point Incremental Forming at High Feed Rates and Rotational Speeds: Surface and Structural Consequences." *CIRP Ann. – Manuf. Technol.*, Vol. 59, pp.311-314 (2010).
- Jeswiet, J., Micari, F., Hirt, G., Bramley, A., Duflou, J., and Al-wood, J., "Asymmetric Single Point Incremental Forming of Sheet Metal." *CIRP Ann. – Manuf. Technol.*, Vol. 54, pp. 623-649 (2005).
- Lasunon, O.U., "Surface Roughness in Incremental Sheet Metal Forming of AA5052." *Adv. Mater. Res.*, Vols. 753-755, pp. 203-206 (2013).
- Li, Y., Daniel, W.J., Liu, Z., Lu, H., and Meehan, P.A., "Deformation Mechanics and Efficient Force Prediction in Single Point Incremental Forming." *J. Mater. Process. Technol.*, Vol. 221, pp. 100-111 (2015).
- Liang, X.W., Shi, L.T., and Ye, Z.B., "Optimization of Polymer Mobility Control for Enhanced Heavy Oil Recovery: Based on Response Surface Method." *J. Pet. Sci. Eng.*, 206, 109065, 2021.
- Lu, B., Chen, J., Ou, H., and Cao, J., "Feature-Based Tool Path Generation Approach for Incremental Sheet Forming Process." *J. Mater. Process. Technol.*, Vol. 213, pp. 1221-1233 (2013).
- Martins, P.A.F., Bay, N., Skjoedt, M., and Silva, M.B., "Theory of Single Point Incremental Forming." *CIRP Ann. – Manuf. Technol.*, Vol. 57, pp. 247-252 (2008).
- Petek, A., Kuzman, K., and Kopac, J., "Deformations and Force Analysis of Single Point Incremental Sheet Metal Forming." *Arch. Mater. Sci. Eng.*, Vol. 35, pp. 107-116 (2009).
- Shim, D.S., "Effects of Process Parameters on Additive Manufacturing of Aluminum Porous Materials and Their Optimization Using Response Surface Method." *J. Mater. Res. Technol.*, Vol. 15, pp. 119-134 (2021).
- Silva, M.B., Skjoedt, M., Martins, P.A.F., and Bay, N., "Revisiting the Fundamentals of Single Point Incremental Forming by Means of Membrane Analysis." *Int. J. Mach. Tools Manuf.*, Vol. 48, pp. 73-83 (2008).
- Song, H., Chung, H.Y., and Nam, K., "Response Surface Modeling with Box-Behnken Design for Strontium Removal from Soil by Calcium-Based Solution." *Environ. Pollut.*, Vol. 274, 116577 (2021).
- Verbert, J., Belkassam, B., Henrard, C., Habraken, A.M., Gu, J., Sol, H., Lauwers, B., and Duflou, J.R., "Multi-step Toolpath Approach to Overcome Forming Limitations in Single Point Incremental Forming." *Int. J. Mater. Form.*, Vol. 1, pp. 1203-1206 (2008).
- Vijayakumar, M.D., Chandramohan, D., and Gopalaramasubramanian, G., "Experimental Investigation on Single Point Incremental Forming of IS513Cr3 Using Response Surface Method." *Mater. Today: Proc.*, Vol. 21, No. 1, pp. 902-907 (2020).
- Yamashita, M., Gotoh, M., and Atsumi, S.Y., "Numerical Simulation of Incremental Forming of Sheet Metal." *J. Mater. Process. Technol.*, Vol. 199, pp. 163-172 (2008).
- Zeng, G., Li, S.H., and Lai, X.M., "Optimization Design of Roll Profiles for Cold Roll Forming

Based on Response Surface Method.” *Mater. Des.*, Vol. 30, No. 6, pp.1930-1938 (2009).

單點增量成型生產錐形杯 之最佳化

吳明昌 賴俊瑋 曹中丞
龍華科技大學機械工程系

廖堉博
國立中央大學機械工程系

摘要

單點增量成型 (SPIF) 是一種經濟、快速的金屬板材成形技術，不需要一套指定且複雜的模具和壓床。使用 ABAQUS 軟體開發增量式金屬板成型錐形杯的有限元素法 (FEM) 模型。透過 SPIF 測量成品錐形杯側壁厚度最薄處 (T) 和均勻度 (U) 上的刀具路徑沖頭的幾何形狀和加工參數。用於實驗設計的 SPIF 變數包括沖頭直徑 (D)、Z 軸進給距離 (Z)、沖頭轉速 (R) 和進給速率 (F)。實驗使用 25 組類似物和 Box-Behnken 設計 (BBD)。Minitab 軟體用於迴歸分析並開發成品錐形杯的 T 和 U 預測方程式。FEM 模型和響應曲面方法 (RSM) 用於確定成品錐形杯的 T 和 U 的最佳設計。與使用 RSM 計算的成品錐形杯的 T 和 U 預測方程式相比，FEM 的結果顯示出出色的準確性。